JMEPEG (2007) 16:635–639
DOI: 10.1007/s11665-007-9079-2

1059-9495/$19.00

The Structure Stability of Carbide-Free Bainite Wheel Steel

Mingru Zhang, Jianqing Qian, and Haicheng Gu

(Submitted January 6, 2006; in revised form August 29, 2006)

Metallographic structures of carbide-free bainite steel wheel rim are mainly composed of supersaturated lath ferrite and retained austenite film among bainitic ferrite laths. It is suspected that supersaturated ferrite and retained austenite are likely to decompose under the influence of temperature change and mechanical stress. Stability of wheel rim structure is studied by means of x-ray diffraction, dye microscopy, and micro-hardness test. When the samples are tempered in the range of 150-350 °C, the retained austenite films are at the state of relative stability. Fifty percent of retained austenite is decomposed when the sample is tempered at 400 °C. Microhardness increases when the sample is tempered at 150 °C. The decrease in hardness is mild when the samples are tempered from 200 to 500 °C. The mechanical stability of retained austenite film is studied with tensile sample under the effect of tensile stress. The retained austenite appears to be stable in low and middle degree of deformation, and decomposition occurs at great amount of deformation. Diffraction peak of carbide is not found in all above experiments. The steel enriched silicon prevents the carbide precipitation during the transformation. It indicates the carbide-free bainite wheel steels have an excellent thermal and mechanical stability.

Keywords carbide-free bainite, dye microscopy, retained austenite, wheel steel

1. Introduction

The performance of wheels influences safety and economy of railway transportation. High-speed coach and heavy wagon with an axle-load of over 23/25 tons require higher safety and reliability. Wheel safety is vital for both heavy load and high speed of railway transportation. In order to improve strength, toughness, and fatigue resistance, it is necessary to optimize the chemical composition, microstructure, and manufacturing technique of wheel materials (Ref 1-5). For a long time, scholars engaged in material research have dedicated to wheel steel study on the alloy design, microalloying, smelting and heat treatment technique, and made an effective achievement with enhanced steel purity and wheel structure uniformity (Ref 6-9).

The common characteristics of above mentioned wheel steels is that they are made of medium and high-carbon steel with the microstructure of pearlite-ferrite. The phase interfaces between carbide and ferrite in pearlite are source of fatigue cracks. Furthermore, high-carbon content facilitates the formation and propagation of thermal crack. Carbide-free bainite steels have excellent mechanical properties, fracture resistance and some extent of wear resistance (Ref 10, 11). The steel of carbide-free bainite can be applied to wheel manufacture, as long as the chemical composition of the wheel can assure the microstructure below wheel tread 50-70 mm is mainly carbide-free bainite. The structure stability of carbide-free bainite wheel has been studied in this paper.

Mingru Zhang and **Haicheng Gu,** State Key Laboratory for Mechanical Behavior of Materials, Xi'an Jiaotong University, Shanxi 710049, P.R. China; **Mingru Zhang** and **Jianqing Qian,** Technical Center, Maanshan Iron & Steel Co., Ltd., Anhui 243000, P.R. China. Contact e-mail: zhangmingru@mgjszx.com.

2. Experimental Procedures

The Si-Mn-Mo carbide-free bainite steel contains sufficient silicon to prevent the precipitation of carbide during transformation at slow cooling rates, sufficient manganese for the purposes to improve hardenability, and some other alloying elements, such as molybdenum and vanadium. The molybdenum and vanadium are useful to gain fine grains, laths, and/or plates, and to repress temper embrittlement (Ref 12, 13). The experimental steel was smelted by intermediate frequency induction furnace at the lab of Maanshan Iron & Steel Co., Ltd., China, and electro-slag re-melted into round ingots with a diameter of 420 mm and a weight of 920 kg. After stress relief annealing, they were rolled into two experimental wheels of 840 mm in diameter. For heat treatment, wheels were heated to 910 °C, and flash quenching was conducted at the wheel rim section by programmed control. Metallographic samples and tensile samples were taken from one of the wheel in rim section under the tread, metallographic samples below the tread 5 mm and the tensile sample below the tread 30 mm. For thermal stability test, only one metallographic sample was used in order to decrease the error in measurement. First, the microstructure of the sample was observed with 4% nitric acid alcohol and dye method simultaneously, the content of retained austenite was determined by X-ray diffractometer, and microhardness was tested; second, the sample was tempered at given temperature ranging from 150 to 500 °C; third, observation of the microstructures, determination of the content of retained austenite and micro-hardness test were conducted again, and

so on. At every tempering temperature, the sample was held 2 h, then cooled to room temperature in the air.

Microstructure of samples was analyzed with microscope Zeiss Axioskop1-MAT; and microhardness with Akashi HM-125. Tensile test was conducted using WAW-Y500A material testing system. The tensile sample was cut into five segments after fracture. Their actual deformations were calculated. All the samples were analyzed by microstructure observation, x-ray diffraction, and micro-hardness measurement. According to microstructure observation, the change of austenite content in the sample tempered at escalating temperatures is evaluated. In the photographs obtained by dye method, the palm yellow or red zone represents the constituent of ferrite, the blue represents the carbide-free bainite, and the white represents the retained austenite or martensite because they are difficult to be etched. The volume fraction of retained austenite also determines by X-ray diffractometer with the diffraction peak integral intensity of {220},{311} crystal plane (Ref 14, 15). The conversion ratio X can be calculated by

$$X = \frac{\gamma_0 - \gamma_\ell}{\gamma_0} \quad \text{(Eq 1)}$$

where γ_0 and γ_ℓ are volume fraction of austenite before and after testing.

3. Results and Analysis

3.1 Thermal Stability

A small amount of retained austenite film (<10%) is observed by x-ray diffraction spectrum and optical microscope in the samples etched with 4% nitric acid alcohol and dye method. The retained austenite content and microhardness after tempered at different temperatures are shown in Table 1 and Fig. 1. The microstructure of the quenching wheel rim is shown in Fig. 2, and others as shown from Fig. 3 to 7. It can be seen that retained austenite remains stable between 150 and 250 °C, and becomes less stable up to 350 °C. Only half of retained austenite decomposed when it was tempered at 400 °C. A small quantity of austenite was still retained until 500 °C. The results of microstructure analyses tally well with the content of retained austenite. When tempering temperature exceeds 350 °C, content of retained austenite reduces with escalating tempering temperature, and lath width of bainite ferrite become wider. Microhardness slightly increases when retained austenite is tempered at 150 °C. The hardness decreases slightly when tempered from 200 to 500 °C.

3.2 Mechanical Stability

The austenite volume fraction and bulk conversion ratio in deformed samples are determined by X-ray diffractometer, as shown in Table 2 and Fig. 8. It can be seen that austenite in the structure basically does not change when deformation is in the range of from 10 to 21%. The austenite conversion is descending smoothly, and the microstructure of 21 and 57% deformation are shown in Fig. 9, i.e., austenite is at stable state when the deformation is at the above range. The austenite conversion is obvious when deformation increases from 21 to 42%. But 2.4% volume fraction of the austenite in the structure has not been changed. About 1% volume fraction of austenite is still retained even when the deformation goes up to 57%.

4. Discussion

The lattice parameter of retained austenite below the wheel rim section measured by means of x-ray diffraction spectrum

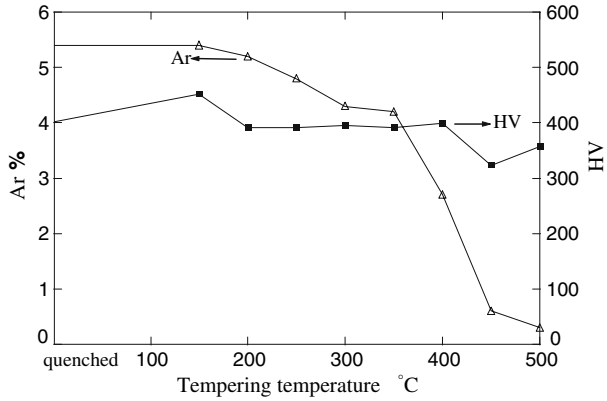

Fig. 1 Retained austenite content, microhardness and tempering temperature curves

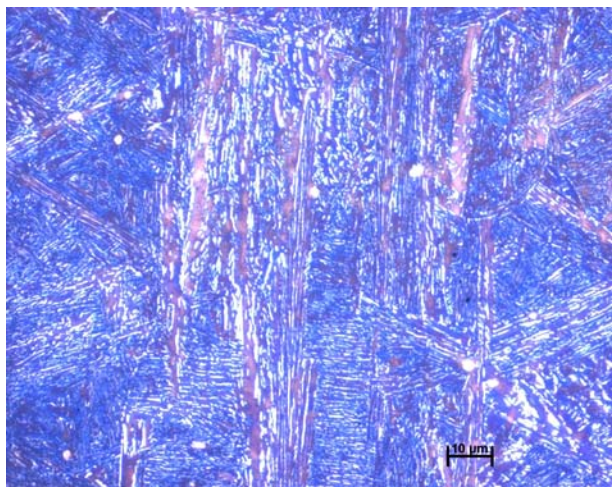

Fig. 2 Microstructure of the flash quenched wheel rim, dye method

Table 1 The retained austenite content and microhardness at different tempering temperature

Item	As quenched	150 °C	200 °C	250 °C	300 °C	350 °C	400 °C	450 °C	500 °C
Microhardness, HV	401	452	392	392	395	391	399	323	357
Ar, %	5.4	5.4	5.2	4.8	4.3	4.2	2.7	0.6	0.3
Austenite conversion ratio X	0	0	0.037	0.11	0.20	0.22	0.50	0.89	0.94

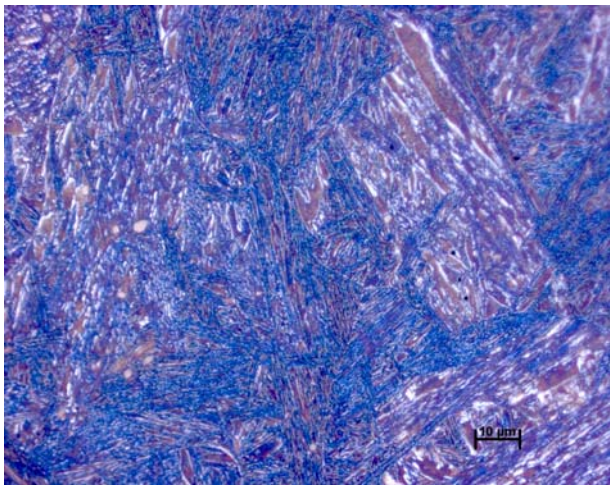

Fig. 3 Microstructure of the wheel rim tempered at 150 °C, dye method

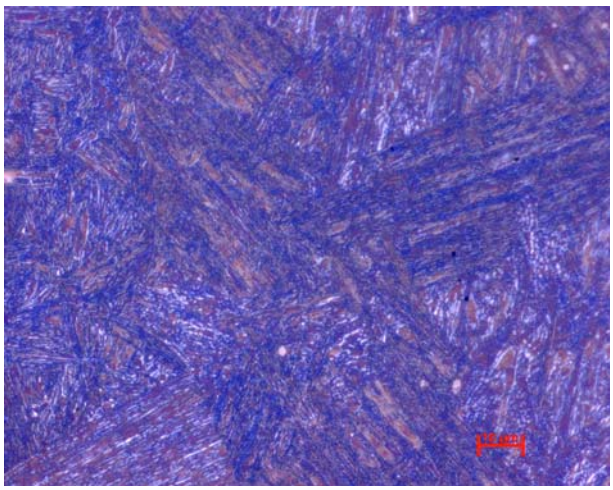

Fig. 4 Microstructure of the wheel rim tempered at 250 °C, dye method

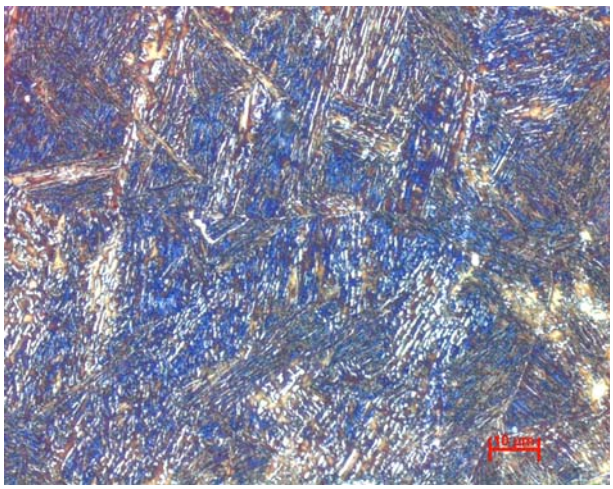

Fig. 5 Microstructure of the wheel rim tempered at 350 °C, dye method

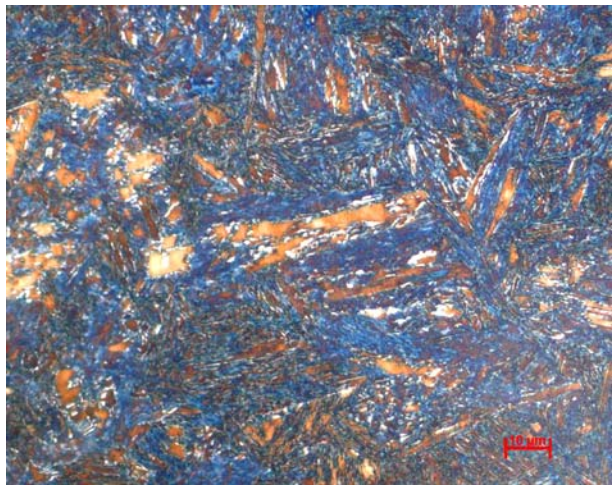

Fig. 6 Microstructure of the wheel rim tempered at 400 °C, dye method

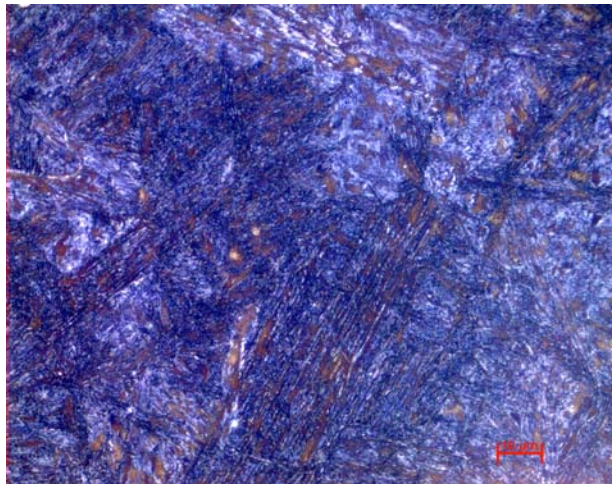

Fig. 7 Microstructure of the wheel rim tempered at 500 °C, dye method

Table 2 The retained austenite content vs. deformation

Deformation, %	0	10	12	21	42	57
Ar, %	9.0	9.0	8.5	6.6	2.4	1.0
Austenite conversion ratio X	0	0	0.06	0.27	0.73	0.89

determination is 0.3614 nm. The relationship between the lattice constant and carbon content can be formulated (Ref 16, 17) as Eq 2:

$$[\mathrm{C}] = \{a_0 - 0.3578 - 0.000096\,[\mathrm{Mn}] + 0.00152\,[\mathrm{Si}] - 0.00031\,[\mathrm{Mo}]\}/0.0033 \quad \text{(Eq 2)}$$

where a_0 is actual lattice parameter of retained austenite, equaling 0.3614 nm; [Mn], [Si] and [Mo] correspond to the weight percents of elements Mn, Si, and Mo in the austenite, respectively. For this steel, carbon content of retained austenite is 1.75 wt.% according to Eq 2. On basis of structure

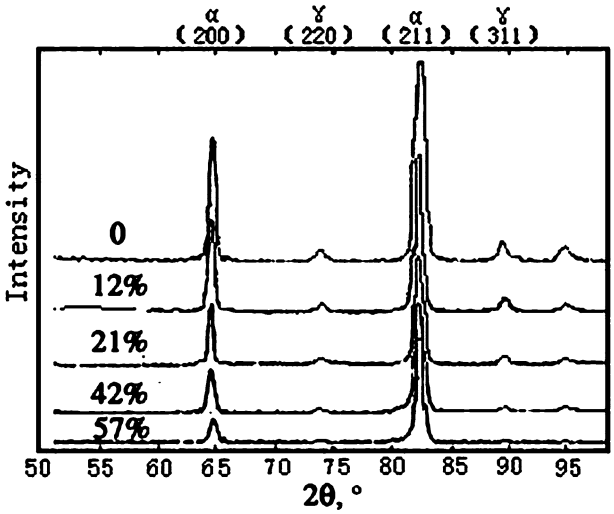

Fig. 8 X-ray diffraction patterns of the samples deformed with different reductions

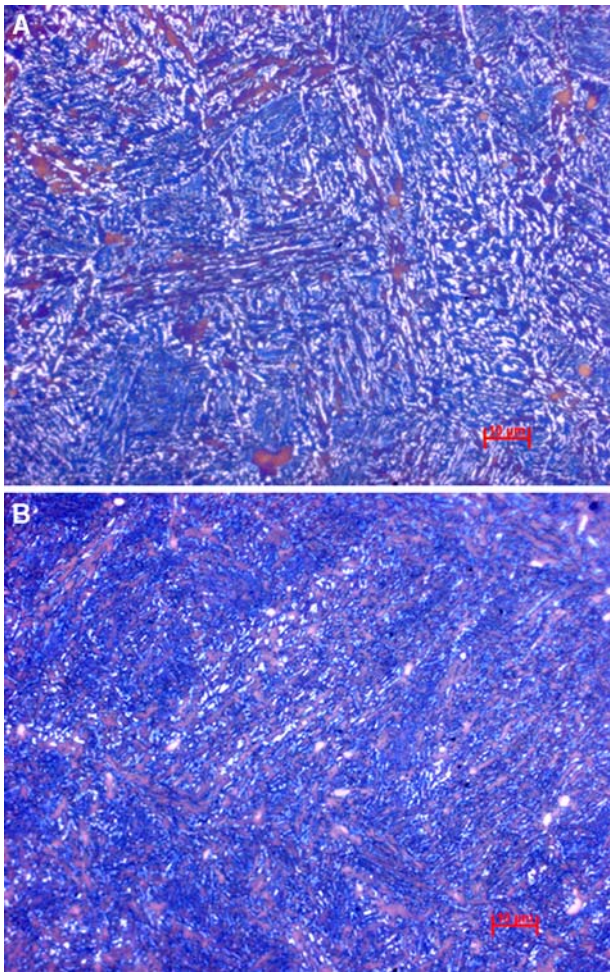

Fig. 9 Relationships between deformation, retained austenite content, and microstructure. (a) 21% of deformation; and (b) 57% of deformation

uniformity of the wheel rim section, it is appropriate that carbon content of retained austenite is 1.6 wt.%. Obviously, retained austenite in the steel belongs to supersaturating austenite of high-carbon content. Once the supersaturating retained austenite turns into high-carbon martensite or precipitates into carbide phase due to deformation stress induced transformations (Ref 18) or critical temperature, it would without doubt bring serious bad influence to safety of the wheel running. Actually, it is found that the addition of silicon inhibits the precipitation of the brittle carbide. By adding appropriate quantity of elements like Mn, as well as correct heat treatment, the retained austenite almost is stable (Ref 19). Silicon makes an effect on controlling precipitation of the brittle carbide, and has contributed to high-concentration carbon in supersaturating austenite and obtains the film-retained austenite that has better stability than that of the blocky retained austenite. Martensite Phase transformation start point M_s is controlled by carbon content of retained austenite. The relationship between the M_s of retained austenite and carbon content of retained austenite is given in literature (Ref 20).

$$M_s\ (^\circ C) = M_s^o - 564(X_c - \bar{X}) \quad \text{(Eq 3)}$$

where M_s^o in the formula is transformation start point of martensite, with average carbon content. X_c is carbon concentration of retained austenite (wt.%). $\overline{X}$ is average carbon concentration (wt.%) in the material.

Correlative parameters of the experimental steel are put into Eq 3 to calculate the M_s. The M_s of retained austenite is −127 °C. When wheel is heated to austenitizing temperature due to heating by braking and then rapidly cooled in a moment, the heating is so fast that the carbon in the original retained austenite has no time to diffuse. Low-carbon austenite is formed in the process of bainite ferrite transformation under the condition of heating, and then transforms into the low-carbon bainite or martensite during natural cooling. While the transformation point M_s of high carbon parts of retained austenite is still −127 °C, they are difficult to take place martensite transformation even at low temperature. Only in the low carbon parts of retained austenite during heating and cooling procedure, phase transformation will occur. The products of phase transformation are still carbide-free bainite and/or low-carbon lath martensite of low-volume fraction. Thus, the retained austenite, especially the film-retained austenite, has no effect on whole performance of wheels.

The retained austenite is strongly hydrogen trapping, and improves hydrogen embrittlement if the retained austenite is stable (Ref 21). Hydrogen embrittlement of the carbide-free bainite wheel steel is studying using slow strain rate testing technique. Stability of carbide-free bainite mainly depends on the stability of retained austenite. The relationship between deformation and austenite content presents descending trend when deformation is ranged from 21 to 42%. But 2.4% volume fraction of austenite in the structure has not been changed, and 1% volume fraction of austenite is still retained even when the deformation up to 57%. It manifests the film-retained austenite has excellent mechanical stability, which is essentially related to the high-silicon contents that effectively retard the precipitation of brittle carbide and control the shapes of the retained austenite. Excellent mechanical stability also relates closely to the concentration of solid solution carbon in retained austenite. If the solid solubility of carbon is higher, the martensite start transformation temperature M_s is lower, and the retained austenite is more stable.

It is known by means of the structure observation of tempered and deformed samples that granular bainite in the

structure gradually increase with escalating tempering temperature and deformation degree. The bainite ferrite laths coarsen during tempering or deformation. The retained austenite turns into granular bainite in the process of tempering and deformation. Though the film-retained austenite among inter-phase turns into granular bainite, it has little effect on material performance.

By the way, the carbide-free bainite wheel steel has been experimentally confirmed to possess excellent combination of strength with toughness, high-fatigue resistance, and good tribological behaviors (Ref 22). The second heat of this kind of new novel wheel steel of 90 tons weight was made in Maanshan Iron & Steel Co., Ltd., and eight trial wheels are running now on a specific railway for testing.

5. Conclusions

- The carbide-free bainite has excellent structural stability. The film-retained austenite is in a correspondingly stable state below 350 °C tempering temperature. The variation extent is increasing over 400 °C. A small quantity of retained austenite is still retained until 500 °C.
- When deformation is at low and middle extent, excellent mechanical stability is obtained for carbide-free bainite steel. 1% volume fraction of austenite is still retained even at great degree of deformation.
- The amount of granular bainite gradually increases and bainite ferrite laths coarsen with escalating tempering temperature and deformation degree.
- Martensite structure and carbide precipitation are not found. According to the transformation products, the film-retained austenite hardly influences safety of train transportation. The wheel of carbide-free bainite steel has excellent thermal and mechanical stability.

References

1. J. Sun, K.J. Sawley, and D.H. Stone, Progress in the Reduction of Wheel Spalling, 12th International Wheelset Congress (China), 1998, p 18–29
2. Z. Yimin, Wheels an Axles of Chinese Railway Locomotive and Car Meeting Challenges of 21st Century, 12th International Wheelset Congress (China), 1998, p 10–13
3. T. Datong, Present Condition and Future Development of Axles and Wheels of Chinese Railways, 12th International Wheelset Congress (China), 1998, p 14–17
4. P.J. Mutton and R. Boelen, Wheel Developments for High Axle Load Operations, 4th International Heavy Haul Railway Conference (Brisbane), 1989
5. S.A. Parsons and D.V. Edmonds, Microstructure and Mechanical properties of Medium-carbon Ferrite Steel Microalloyed with Vanadium, *Mater. Sci. Technol.*, 1987, **3**(11), p 894–904
6. U.P. Singh, B. Roy, S. Jha, and S.K. Bhattacharry, Microstructure and Mechanical Properties of as Rolled High Strength Bainitic Rail Steels, *Mater. Sci. Technol.*, 2001, **17**(1), p 33–38
7. P. Cassidy, A New Wheel Material for the New Century, 13th International Wheelset Congress (Rome), 2001
8. S.E. Offerman, N.H. van Dijk, M.Th. Rekveldt, J. Sietsma, and S. van der Zwaag, Ferrite/Pearlite Band Formation in Hot Rolled Medium Carbon Steel, *Mater. Sci. Technol.*, 2002, **18**(3), p 297–303
9. U.P. Singh, A.M. Popli, D.K. Jain, B. Roy, and S. Jha, Influence of Microalloying on Mechanical and Metallurgical Properties of Wear Resistant Coach and Wagon Wheel Steel, *J. Mater. Eng. Perform.*, 2003, **12**(5), p 573–580
10. F.G. Caballero, H.K.D.H. Bhadeshia, K.J.A. Mawella, D.G. Jones, and P. Brown, Very Strong Low Temperature Bainite, *Mater. Sci. Technol.*, 2002, **18**, p 279–284
11. T. Constable, R. Boelen, and E.V. Pereloma, The Quest for Improved Wheel Steels Enters the Martensitic Phase, 14th International Wheelset Congress (USA), Oct 2004
12. A. Ali, Bainitic Microstructures Formed by Split Isothermal Transformation in an Fe-C-Si-Mn-Mo Steel, *Metallur. Mater. Trans. A*, 1996, **27A**(5), p 1141–1147
13. A. Zarei Hanzaki, P.D. Hodgson, and S. Yue, Retained Austenite Characteristics in Thermomechanically Processed Si-Mn Transformation-Induced Plasticity Steels, *Metallur. Mater. Trans.*, 1997, **28A**(11), p 2405–2414
14. K. Tohji and Y. Udagawa, Double-crystal Spectrometer for Laboratory EXAFS Spectroscopy, *J. Rev. Sci. Instrum.*, 1988, **59**(7), p 1120–1127
15. A.T. Shuvaev, B.Y. Helmer, and T.A. Lyubeznova, et al., Laboratory Diffractometer-based XAFS Spectrometer, *J. Synchrotron Rad.*, 1999, **6**, p 158–160
16. A. Airod, and R. Petrov, et al., Analysis of the Trip Effect by Means of Axisymmetric Compressive Tests on a Si-Mn Bearing Steel, *ISIJ Int.*, 2004, **44**(1), p 179–180
17. S.S. Babu, E.D. Specht, S.A. David, E. Karapetrova, P. Zschack, M. Peet, and H.K.D.H. Bhadeshia, In-situ Observation of Lattice Parameter Fluctuations in Austenite and Transformation to Bainite, *Metallur. Mater. Trans. A*, 2005, **36A**(12), p 3281–3289
18. C.Y. Huo and H.L. Gao, Strain-induced Martensitic Transformation in Fatigue Crack Tip Zone for a High Strength Steel, *Mater. Character.*, 2005, **55**, p 12–18
19. M.Y. Sherif, C. Garcia Mateo, T. Sourmail, and H.K.D.H. Bhadeshia, Stability of Retained Austenite in TRIP-assisted Steels, *Mater. Sci. Technol.*, 2004, **20**(3), p 319–322
20. G.I. Rees and H.K.D.H. Bhadeshia, Bainite Transformation Kinetics Part 1 Modified Model, *Mater. Sci. Technol.*, 1992, **8**(11), p 985–993
21. H.K. Yalci and D.V. Edmonds, The Effect of Hydrogen on the Bainite Transformation, *J. Mater. Sci.*, 1999, **34**, p 711–717
22. M. Zhang, L. Chen, and H. Gu, Microstructure and Mechanical Properties of Carbide-free Bainite Railway Wheels Produced by Programmed Quenching (to be published)